ORIGINAL ARTICLE

Reproductive Medicine and Biology | Open Access | **WILEY**

TSNAXIP1 is required for sperm head formation and male fertility

Tasrin Sultana[1] | Tokuko Iwamori[2] | Naoki Iwamori[1,2] 🔘

[1]Laboratory of Zoology, Graduate School of Bioresource and Bioenvironmental Sciences, Kyushu University, Fukuoka, Japan

[2]Laboratory of Zoology, Graduate School of Agriculture, Kyushu University, Fukuoka, Japan

Correspondence
Tokuko Iwamori and Naoki Iwamori, Laboratory of Zoology, Graduate School of Agriculture, Kyushu University, 744 Motooka, Nishi-ku, Fukuoka-shi, Fukuoka 819–0395, Japan.
Email: tokuko@agr.kyushu-u.ac.jp and iwamori@agr.kyushu-u.ac.jp

Abstract

Purpose: TRANSLIN (TSN) and its binding partner TSNAX have been reported to contribute to a wide spectrum of biological activities including spermatogenesis. TSN accompanies specific mRNA transport in male germ cells through intercellular bridges. A testis-expressed protein TSNAXIP1 was reported to interact with TSNAX. However the role of TSNAXIP1 in spermatogenesis remained unclear. This study aimed to elucidate the role of TSNAXIP1 in spermatogenesis and male fertility in mice.

Methods: TSNAXIP1 knockout (KO) mice were generated using the CRISPR-Cas9 system. The fertility, spermatogenesis, and sperm of TSNAXIP1 KO males were analyzed.

Results: TSNAXIP1, and especially its domains, are highly conserved between mouse and human. *Tsnaxip1* was expressed in testis, but not in ovary. TSNAXIP1 KO mice were generated, and TSNAXIP1 KO males were found to be sub-fertile with smaller testis and lower sperm count. Although no overt abnormalities were observed during spermatogenesis, lack of TSNAXIP1 induced sperm head malformation, resulting in a unique flower-shaped sperm head. Moreover, abnormal anchorage of the sperm neck was frequently observed in TSNAXIP1 null sperm.

Conclusion: A testis-expressed gene TSNAXIP1 has important roles in sperm head morphogenesis and male fertility. Moreover, TSNAXIP1 could be a causative gene for human infertility.

KEYWORDS
gene editing, spermiogenesis, sperm head, infertility, TSNAXIP1

1 | INTRODUCTION

Spermatogenesis is the complex biological process of cellular transformation that begins with diploid spermatogonial stem cells. After mitosis to increase cell numbers, spermatogonia enter the meiotic phase of spermatocytes to produce haploid spermatids. Haploid spermatids undergo a morphological transformation, called spermiogenesis to generate mature spermatozoa.[1,2] Spermiogenesis involves acrosome formation, nuclear elongation, and tail formation.[3]

Proteins predominantly expressed in post-meiotic germ cells are considered to be involved in spermiogenesis including the conversion of nucleosomal basic proteins.[4] Defects in spermiogenesis manifest in male fertility defects, such as low sperm count, sperm deformation, and poor sperm motility.[3]

TSNAXIP1 (Translin-associated factor X (TSNAX)-interacting protein 1) is predominantly expressed in the post-meiotic stages of male germ cells.[5] The gene is located on the long arm of chromosome 8 in mice. Its transcript has 16 coding exons, translating into a

704 amino acid residue protein, having a predicted molecular weight of 81 kDa. TSNAXIP1 is conserved across all groups from invertebrates to vertebrates. Bioinformatic analysis showed that mouse TSNAXIP1 has an SMC (structural maintenance of chromosomes) domain (131-351aa) and a TSNAXIP_N domain (101-202aa) (https://www.ncbi.nlm.nih.gov/protein/EDL11315.1).

TSNAXIP1 interacts with TSNAX, which was reported to interact with three novel testis-expressed proteins MEA-2, SUN1, and AKAP9 in a yeast two-hybrid system and GST (glutathione S-transferase) pull-down experiments.[5] All three proteins have specific roles in spermatogenesis. MEA-2 is thought to maintain Golgi structure and is indispensable for mouse spermatogenesis, SUN1 plays a role in telomere interaction and synapsis between the leptotene and diplotene stages during meiotic prophase I, and AKAP9 contributes to maintain homeostasis of the cytoskeleton in germ cells and the ectoplasmic specialization which creates the adhesion between Sertoli cells and germ cells.[6–8] Moreover, TSNAX is also a binding partner of TRANSLIN (TSN), which is a DNA-binding protein.[9] Testis brain–RNA-binding protein (TB-RBP), the mouse ortholog of TSN, transports specific mRNAs from nuclei into intercellular bridges (ICB) in mouse male germ cells.[10] TB-RBP also plays a role in spermatogenesis, since TB-RBP null mice showed abnormal spermatogenesis and lower sperm count.[11] The interactions among TSN, TSNAX, and TSNAXIP1, together with the expression pattern of TSNAXIP1 in post-meiotic germ cells, suggest that TSNAXIP1 has a potential role in spermatogenesis. In this study, we have disrupted TSNAXIP1 in mice using Clustered Regulatory Interspaced Short Palindromic Repeats and CRISPR-associated protein 9 (CRISPR-Cas9) genome editing technology to investigate the role of TSNAXIP1 in spermatogenesis and male fertility.

2 | MATERIALS AND METHODS

2.1 | Animals

Mice were purchased from CLEA Japan Inc. (Tokyo, Japan) or SLC Inc. (Shizuoka, Japan). ICR strain was used to analyze expression of *Tsnaxip1* in multiple tissues. To generate TSNAXIP1 KO mice, B6D2F1 mice were used to obtain fertilized eggs.

2.2 | Multiple sequence alignment

Peptide sequences of TSNAXIP1 orthologs were obtained from the NCBI database (https://www.ncbi.nlm.nih.gov). The sequence IDs for mouse, rat, human, chimpanzee, and zebrafish TSNAXIP1 are EDL11315.1, NP_001102600.1, AAI11019.1, XP_009429333.1, and XP_009291852.1 respectively. Then sequences were aligned using Multalin version 5.4.1 (http://multalin.toulouse.inra.fr/multalin/) and protein BLAST (https://blast.ncbi.nlm.nih.gov/Blast.cgi?PAGE=Proteins).

2.3 | Semi-quantitative and quantitative reverse transcription-polymerase chain reaction (RT-PCR)

Total RNAs were extracted from multiple tissues isolated from adult WT (wild type) mice using ISOGEN (Nippon Gene, Tokyo, Japan), followed by reverse transcription using SuperScript™ IV Reverse Transcriptase (Thermo Fisher Scientific). *Gapdh* was used as an internal control. For quantitative PCR (qPCR), KAPA SYBR FAST qPCR Master Mix (Kapa Biosystems) and 7500 Fast Real-time PCR system (Applied Biosystems) were used. The data were then analyzed using the comparative Ct method using *Gapdh* as the internal control. Primers used in this study are listed in Table 1.

2.4 | Generation of TSNAXIP1 KO mice

TSNAXIP1 knockout (KO) mice were generated using the CRISPR-Cas9 system. Two guide RNAs (gRNAs) without off-target sites were designed using CHOPCHOP software (https://chopchop.cbu.uib.no). gRNAs are listed in Table 1. After hybridization of each gRNA (crRNA; IDT) with tracrRNA (IDT), each hybridized gRNA was incubated with Cas9 protein (IDT) to form gRNA/Cas9 ribonucleoprotein complex. The ribonucleoprotein complexes were electroporated into fertilized eggs using NEPA21 Super Electroporator (Nepagene). Treated embryos at the two-cell stage were transplanted into the oviducts of pseudo-pregnant ICR females. The genotype of the pups was determined by genomic PCR using the tail tip. The deletion of the genome was confirmed by Sanger sequencing. In this study, homozygous deletion of *Tsnaxip1* in mice was indicated by KO.

2.5 | Western blot

To detect TSNAXIP1 protein in WT and KO testes, testes were homogenized with RIPA lysis buffer (150mM NaCl, 50mM Tris–HCl, pH 8.0, 1% Nonidet P-40, 0.5% Sodium deoxycholate, and 0.1% SDS), and the amount of total protein in lysate was quantified using BCA protein assay kit (Thermofisher Scientific). Fifty micrograms of protein from each sample were separated with SDS-PAGE, followed by transfer onto PVDF membrane. After blocking with 5% skimmed milk in PBS, Rabbit anti-TSNAXIP1 (1:600 dilution) (a kind gift from Dr. Ikawa, Osaka University), and mouse anti- γ-TUBULIN (1:1000 dilution) (Proteintech) were used as primary antibodies. Blot images were captured and analyzed using VersaDoc™ 5000 MP (Bio-Rad) and Quantity One software (Bio-Rad).

2.6 | Breeding test

To evaluate the fertility of TSNAXIP1 KO males, 8-week-old male KO mice were housed individually with 8-week-old WT female mice for 2months. The number of pups and copulation plugs were checked daily.

TABLE 1 List of primers used in this study.

Target	Forward (5′-3′)	Reverse (5′-3′)	Purpose
Tsnaxip1	CTCAAGACCACCTT TCCTCT	CTTCTCCTCATCCT CCAGT	RT-PCR
Gapdh	GTGCTGAGTATGTCGTG GAGTC	CATACTTGGCAGGTTTC TCCAG	RT-PCR, RT-qPCR
Tsnaxip1	TAAGCCCTTGCAGTTAT CCTTG	TGTCCTGGAACAATACC TAGCC	Genotyping
Tsnaxip1	GCAGTCTCATATGGAAG CAGTG	TTGGTAGTGGAGTCACA ACAGG	
Tsnaxip1	AGCATCTCCAAGCC CAAGTA	CTCAGTTCCTGTGCAGA ATCC	RT-qPCR
Tsnax	GGAAGCATGACACC TTCCCA	CATATTTGTCGTGC CTGGCG	
Tsn	GAGCTGGATTCTGG TTTTCG	TCATAGACCACCTC CTCTAC	
Tsnaxip1 (Exon 4–5)	AGCATCTCCAAGCC CAAGTA	TCGTACGCATTCTT GATGGA	RT-PCR
Tsnaxip1 (Exon 1–16)	GCCAACCTACAGGA GCGTAA	TCTGGCTCTCGTGG TCCTAC	
Tsnaxip1	GGAATCGAGCCAAGTAA GCGAGG		gRNA1
	CTCGTACGCATTCTTGA TGGAGG		gRNA2

2.7 | Analysis of sperm morphology

After dissection, cauda epididymis was cut in small pieces in a drop of prewarmed TYH medium (LSI medience co) and placed under 5% CO_2 at 37°C in a humidified incubator for 30 min. The number of motile sperm released from epididymis was counted as a concentration using a hemocytometer ($n=5$). For each mouse, sperm count was repeated three times. To evaluate the morphology of sperm, spermatozoa were smeared on glass slides and fixed with 2% Paraformaldehyde (Fujifilm Wako) in PBS. To analyze sperm heads, the nucleus and acrosome were visualized by DAPI and rhodamine-conjugated peanut agglutinin (PNA) staining,[12] respectively, and observed using a fluorescent microscope (BZ-X700; Keyence). A minimum of 200 sperms from each mouse ($n=3$) were analyzed.

2.8 | Histological analysis of testis and epididymis

After the weight of each testis was measured, testes and epididymides were fixed in Bouin's fixative (Polysciences, Inc.) and embedded in paraffin (Paraplast; Leica Biosystems). Five micrometer thick sections were deparaffinized and stained using hematoxylin and eosin Y (H&E) (Fujifilm Wako), and the nucleus and the acrosome were stained with SYTOX orange and Alexa488-conjugated PNA (Thermofisher Scientific), respectively, to analyze acrosome formation, and images were captured using a microscope (BZ-X700;

Keyence). For morphometric evaluation, cross-sectional area of seminiferous tubules ($n=3$) were measured using ImageJ software (https://imagej.net/).

2.9 | In vitro fertilization (IVF)

Female B6D2F1 mice (SLC Japan inc.) were superovulated by intra-peritoneal injection of 7.5 IU pregnant mare serum gonadotropin, followed 48 h later by 7.5 IU human chorionic gonadotropin (hCG). Ovulated oocytes were collected 15–16 h after hCG injection from the ampullae of the oviducts into TYH medium. Spermatozoa were obtained from cauda epididymis of WT or TSNAXIP1 null males and preincubated for 1 h at 37°C in TYH medium and added to the medium containing the oocytes at a concentration of 150 sperm/μL. The number of two-cell stage embryos was counted at 24 h after insemination.

2.10 | Statistical analysis

All data were analyzed using GraphPad Prism (Version 5.04). An unpaired t-test was used to analyze the difference between two groups. Differences were considered statistically significant if the p values were less than 0.05 (*), 0.01 (**), 0.001 (***), or 0.0001 (****). Data represent mean ± standard error mean (SEM).

3 | RESULTS

3.1 | *Tsnaxip1* is expressed in testis, but not in ovary

In an alignment of peptide sequences, mouse TSNAXIP1 showed 90.64%, 77.36%, 72.05%, and 35.88% sequence similarity with its rat, human, chimpanzee, and zebrafish orthologs respectively (Figure 1A), indicating that TSNAXIP1 is highly conserved within mammals. TSNAXIP1 has two domains: the SMC domain and the TSNAXIP N-terminal domain (TSNAXIP_N). SMC and TSNAXIP_N domains are 85.5% and 88.2% conserved between mouse and human, respectively (Figures S1 and S2), suggesting that both domains in TSNAXIP1 may be functionally important.

Expression of *Tsnaxip1* in mouse was analyzed using RT-PCR. As shown in Figure 1B, from the twelve tissues tested *Tsnaxip1* was only expressed in the lung, salivary gland, and testis, and was absent from the ovary.

3.2 | Generation of TSNAXIP1 KO mice

To investigate the physiological role of TSNAXIP1, TSNAXIP1 KO mice were generated using the CRISPR-Cas9 system. Two gRNAs were used to delete the specific genome region between exon 3 and exon 5 (Figure 2A), which includes the SMC domain. The deletion was confirmed by genomic PCR and sequencing. When primer pairs flanking each target site of gRNAs, 1F and 1R or 2F and 2R, were used, clear bands were detected in WT but not in KO mice (Figure 2B). When 1F and 2R primer pairs flanking both two gRNAs were used, a single 1.7 kb band was detected in WT, but a much smaller PCR product was detected in KO, indicating that about 1.5 kb of genomic DNA between the two gRNA locations was deleted (Figure 2B). Sequencing data clearly showed that 1519 bp of genomic DNA between exon 3 and exon 5 of *Tsnaxip1* was precisely deleted in the KO allele (Figure 2C). The absence of 75 kDa of TSNAXIP1 protein in the KO testis was confirmed by a western blot analysis (Figure 2D).

To confirm expressions of splicing variants of *Tsnaxip1*, full length *Tsnaxip1* expression was examined by RT-PCR, resulting that a truncated form of *Tsnaxip1* was found to be expressed in the TSNAXIP1 null testis (Figure S3A). Sequencing of the truncated form of *Tsnaxip1* revealed that a short form of TSNAXIP1 without domains could be expressed in the TSNAXIP1 null testis (Figure S3B,C). This result also suggest that the smaller bands detected in western blot could be a non-specific protein but not a splicing variant of TSNAXIP1 (Figure 2D).

Next, the expression of *Tsnaxip1* and its possible interactors, *Tsn* and *Tsnax*, were determined in 8-week-old WT, and 8- and 20-week-old KO testes (referred as KO1 and KO2, respectively) using RT-qPCR. As expected, *Tsnaxip1* expression was not detected in either KO sample using primer pair designed in the SMC domain of *Tsnaxip1*. However, the expression of both *Tsnax* and *Tsn* was similar in all samples even in the absence of TSNAXIP1 in the KO strain (Figure 2E).

3.3 | TSNAXIP1 deficiency induces male subfertility

TSNAXIP1 KO mice were viable and visual observation showed that the growth and behavior of TSNAXIP1 KO mice were normal. To determine whether TSNAXIP1 was required for male fertility, WT or TSNAXIP1 KO males were crossed with WT females. Although the frequency of plug formation was comparable between WT and KO, the average litter size from WT males was 9.2 ± 0.8 and that of KO males was 1.4 ± 0.6, suggesting that TSNAXIP1 KO males may be sub-fertile (Figure 3A). Moreover, the TSNAXIP1 null testis was smaller than the WT testis (Figure 3B). The ratio of testis weight and body weight of the KO mice (average $1.886 \pm 0.3758 \, \text{mg g}^{-1}$) was significantly lower than that of WT (average $3.11 \pm 0.3213 \, \text{mg g}^{-1}$) (Figure 3C and Table S1), suggesting that spermatogenesis could be affected by the lack of TSNAXIP1. To determine whether the sub-fertile phenotype of TSNAXIP1 KO male was associated with spermatogenesis, the histology of the testes was compared. H & E staining of the testes showed that TSNAXIP1 KO spermatogenesis looked normal, although the cross-sectional area of the TSNAXIP1 KO seminiferous tubule was smaller than that of WT tubules (Figure 3D). The area of seminiferous tubule sections in TSNAXIP1 null testes was $3.053 \pm 0.068 \times 10^4 \, \mu\text{m}^2$ ($n=3$), whereas that in WT was $5.040 \pm 0.629 \times 10^4 \, \mu\text{m}^2$ ($n=3$) (Figure 3E). Although the seminiferous tubules in TSNAXIP1 null testes were about half of those in WT, all types of germ cells were observed in the testes lacking TSNAXIP1. Surprisingly, only a few sperm were present in the TSNAXIP1 KO epididymis, although the WT epididymis was filled with mature spermatozoa (Figure 3D).

Since TSNAXIP1 KO males were found sub-fertile, IVF was performed to determine the fertilization ability of TSNAXIP1 null sperm. The ratio of two-cell stage embryos fertilized with TSNAXIP1 null sperm ($29.46 \pm 16.28\%$) was significantly lower than that with WT sperm ($87.72 \pm 2.01\%$) (Figure 3F), suggesting that low litter size from TSNAXIP1 null males could be attributed to the fertilization ability of the sperm lacking TSNAXIP1.

3.4 | TSNAXIP1 deficiency causes oligospermia and defects in the sperm head

The number of cauda epididymal sperm was counted, and the number of sperm in KO epididymis (average $1.47 \pm 0.3053 \times 10^6$ sperms/mL; $n=5$) was found to be about half of that in WT epididymis (average $3.55 \pm 0.3128 \times 10^6$ sperms/mL; $n=5$) (Figure 4A). Sperm morphology was assessed visually, and sperm with flower-shaped head were frequently detected by the lack of TSNAXIP1 (Figure 4B). Such flower-shaped heads were never observed in WT sperm but occurred in $23.63 \pm 3.619\%$ of KO sperm (Figure 4C). The KO
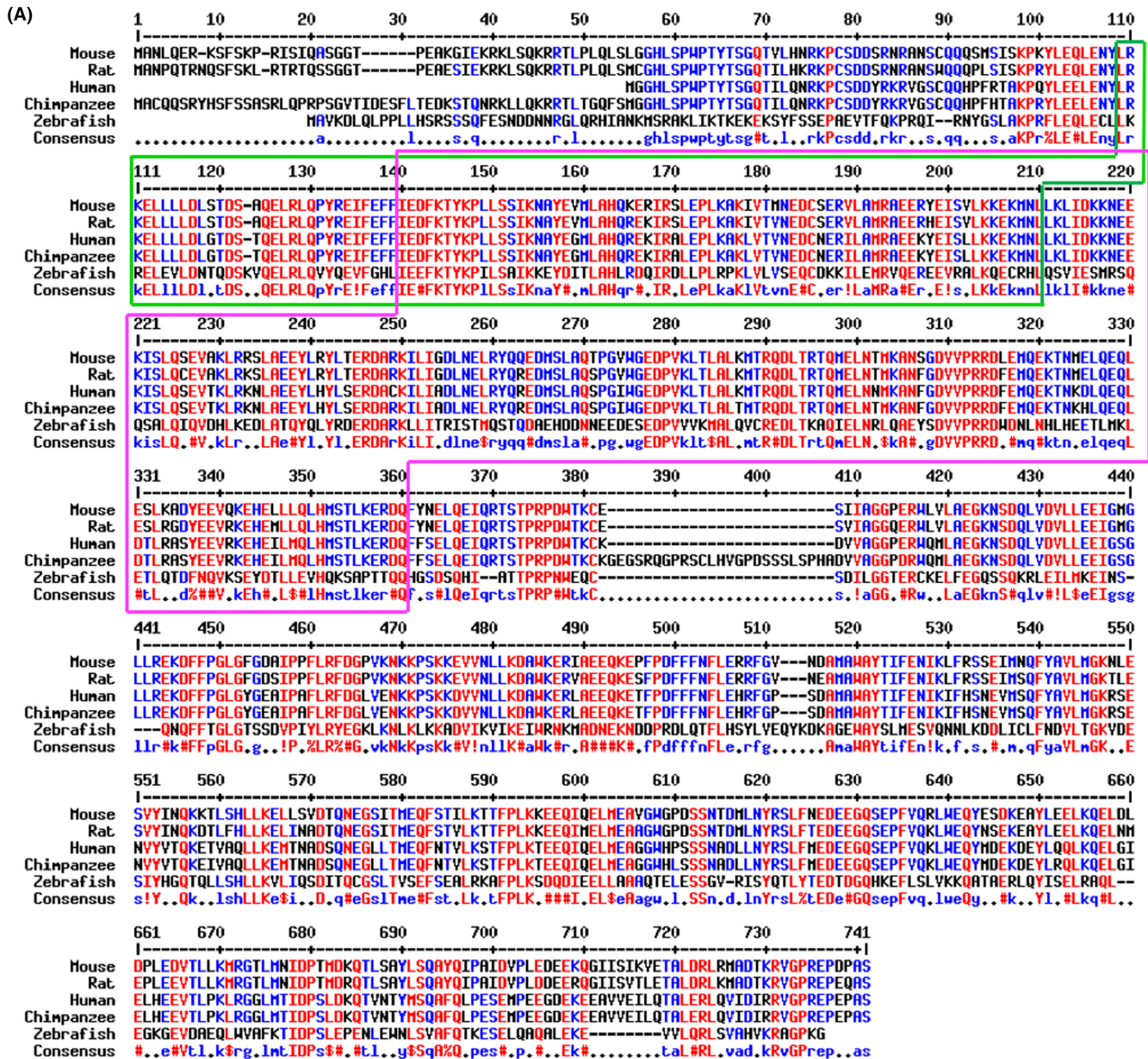
(A)

(B)

FIGURE 1 *Tsnaxip1* is a testis expressed gene. (A). Peptide sequences alignment of different TSNAXIP1 orthologs. Red: High consensus color, Blue: Low consensus color, and Black: Neutral color.! is either I or V, $ is either L or M, % is either F or Y, and # is either N,D,Q or E. Area outlined in green represents the TSNAXIP_N domain and area outlined in pink represents the conserved region of the SMC domain. (B). Expression analysis of mouse *Tsnaxip1* by semi-quantitative RT-PCR of 12 different mouse tissues. *Gapdh* was used as an internal control. B, brain; He, heart; Ki, kidney; LI, large intestine; Li, liver; Lu, lung; Ov, ovary; SG, salivary gland; SI, small intestine; Sp, spleen; St, stomach; Te, testis.

flower-shaped head sperm all had an abnormal anchorage of the neck (also known as the connecting piece or head-tail coupling apparatus) onto the middle of the head (Figure 4B,E). This abnormal head–neck junction was also observed in some KO sperm which had

normal-shaped heads (Figure 4D). On average, $34.73 \pm 2.33\%$ of all KO sperm (with both normal and flower-shaped heads) had abnormal head–neck junctions (Figure 4D). Since the acrosome plays an essential role in shaping of spermatid head,[13] we analyzed the formation of
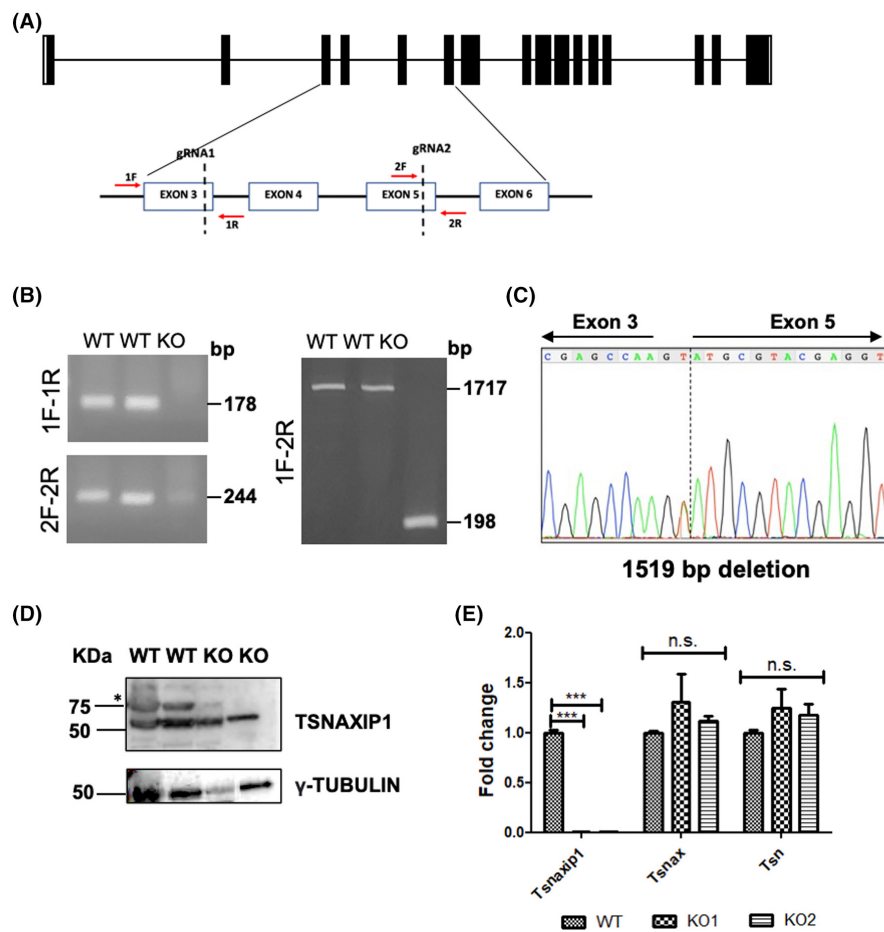
(A)

(B)

(C)

(D)

(E)

FIGURE 2 Generation of TSNAXIP1 KO mice. (A). Schematic representation of genome editing to generate TSNAXIP1 KO mice. Two gRNAs were used targeting between exon 3 and exon 5, respectively. Red arrows indicate primer pairs (1F-1R and 2F-2R) that were used to amplify the targeted regions. (B). Genotyping PCR using 1F-1R, 2F-2R, and 1F-2R primer pairs to confirm KO. (C). Genomic sequence chromatogram of TSNAXIP1 KO mice. (D). Western blot result of TSNAXIP1 protein expression in WT and KO testis. γ-TUBULIN was used as loading control. Asterisk indicates TSNAXIP1 protein. (E). RT-qPCR analysis of testis extracts from adult WT and TSNAXIP1 KO mice (KO1 and KO2 were 8- and 20-weeks old, respectively) for *Tsnaxip1*, *Tsnax*, and *Tsn*. Fold change was normalized to *Gapdh*. Data are presented as mean ± SEM. n.s.: not significant. ***$p < 0.001$.

the acrosome in flower-shaped head sperm of TSNAXIP1 KO using PNA staining to visualize the acrosome. Although an acrosome was present in the flower-shaped head sperm, the shape of the acrosome was distorted aligning with the head shape abnormalities (Figure 4E). Since no abnormality of the acrosome formation was observed in TSNAXIP1 null testes, distorted acrosome in flower-shaped head sperm could be a subsequent effect of abnormal sperm head morphology (Figure S4). The flower-shaped head sperm may not be able to fertilize and the frequency of sperm with flower-shaped heads and abnormal head–neck junction could contribute to the subfertility of TSNAXIP1 null males.

4 | DISCUSSION

In this study, we have shown that TSNAXIP1 is expressed in the lung, salivary gland and testis but not in the ovary (Figure 1B). In a previous study, *Tsnaxip1* transcript was predominantly detected in round spermatids and condensing spermatids of mice.[5] Possibly the greater sensitivity of the RT-PCR detection we used enabled us to detect expression at lower levels in other tissues. In the previous study, GFP-TSNAXIP1 expressed in NIH 3 T3 fibroblasts was localized in the cytoplasm with a concentration around the nucleus.[5] Since proteins having predominant expression in post-meiotic germ cells could have roles in chromatin condensation and sperm development and

maturation,[4] TSNAXIP1 could play a role in spermiogenesis. There are two domains in the TSNAXIP1: the SMC domain, which is highly conserved from bacteria to human and has roles in chromosome organization and segregation,[14] and TSNAXIP_N, which is shared among four TSNAXIP family proteins. Although full-length amino acids are 77.36% conserved between mouse and human TSNAXIP1 (Figure 1A), the SMC domain is 85.5% conserved and TSNAXIP_N is 88.2% conserved (Figures S1 and S2), suggesting that both domains in TSNAXIP1 could have an important function. Since both domains of TSNAXIP1 are highly conserved between mouse and human, TSNAXIP1 was disrupted by CRISPR-Cas9 to investigate the role of TSNAXIP1 during spermatogenesis (Figure 2).

TSNAXIP1 deficiency affected male fertility and an average litter size derived from TSNAXIP1 KO males was below 2, suggesting that TSNAXIP1 null males were sub-fertile (Figure 3A). Furthermore, the size of the TSNAXIP1 null testis was small and the number of sperm in the epididymis was reduced by the lack of TSNAXIP1 (Figure 3B–D). When spermatogenesis without TSNAXIP1 was examined, there were no obvious defects detected in the TSNAXIP1 deficient seminiferous tubules except for the size of sectional areas (Figure 3D,E). Since all kinds of male germ cells were observed even in TSNAXIP1 null seminiferous tubules, TSNAXIP1 might not affect the differentiation of male germ cells. However, the TSNAXIP1 null epididymis contained only a few sperm (Figure 3D), suggesting that TSNAXIP1 could have a role during spermiogenesis or in the release of sperm

FIGURE 3 TSNAXIP1 deficiency causes male subfertility in mice. (A). The average litter size was measured for WT and KO male mice (n = 5). (B). Representative images of WT and KO testes. Scale bar 2 mm. (C). Testis weight per body weight of WT and KO mice (n = 5). (D). Representative micrographs of H&E staining of testicular sections from 8 week and epididymis from 12-week-old WT and KO mice. Scale bar 50 μm. (E). Measurement of seminiferous tubule cross-sectional area (n = 3). F. IVF analysis in WT and KO using cumulus-intact oocytes (n = 3). Data are presented as mean ± SEM. $*p < 0.05$, $**p < 0.01$, $***p < 0.001$, $****p < 0.0001$.
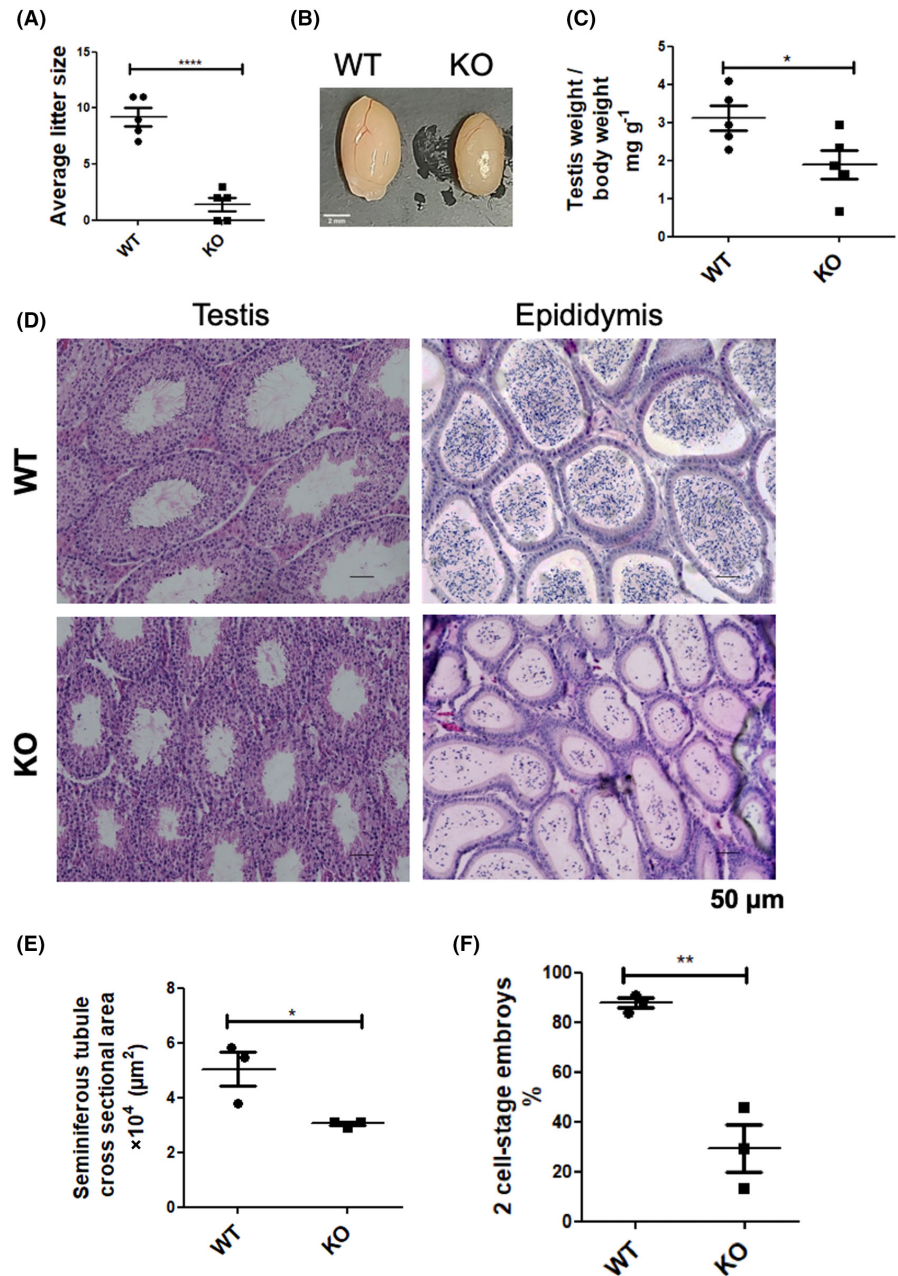
from Sertoli cells into the lumen of the seminiferous tubules. To determine the relationship between the litter size and the fertilization ability of sperm lacking TSNAXIP1, IVF was performed. As a result of IVF, the ratio of two-cell stage embryos, which were fertilized with TSNAXIP1 null sperm, was significantly lower (Figure 3F). Since the litter size derived from TSNAXIP1 null male and the ratio of two-cell stage embryos derived from TSNAXIP1 null sperm were comparable, sub-fertility of TSNAXIP1 deficient male could be attributed to the ability but not the reduced count of their sperm.

In addition to the reduced sperm count, sperm with abnormal head-shapes were frequently detected in the TSNAXIP1 null epididymis (Figure 4B). Around 23% of sperm had abnormal head morphology, with a flower-shaped appearance (Figure 4C). About 34% of sperm had an abnormality in the connecting piece anchorage (Figure 4D). The connecting piece is thought to regulate

sperm motility partly.[15] On the other hand, almost all sperm from TSNAXIP1 KO mice had normal tails and tail lengths were comparable to those of WT sperm (Figure 4B), suggesting that TSNAXIP1 could be important for the head formation of sperm rather than tail formation. As a result of these defects, the number of healthy sperm in the TSNAXIP1 KO male is much lower than in WT and could result in oligospermia (Figure 4A). Although we could not obtain an immunostaining compatible antibody against TSNAXIP1 and the localization of TSNAXIP1 in sperm remains unknown, TSNAXIP1 could have a role in the morphogenesis of the sperm head. Since TSNAXIP1 is well conserved between mouse and human as discussed above, TSNAXIP1 might be a causative gene for human infertility such as oligospermia and abnormal sperm morphology.

Recently, another group reported phenotypes in spermatogenesis in the absence of TSNAXIP1.[16] Of note, there are some
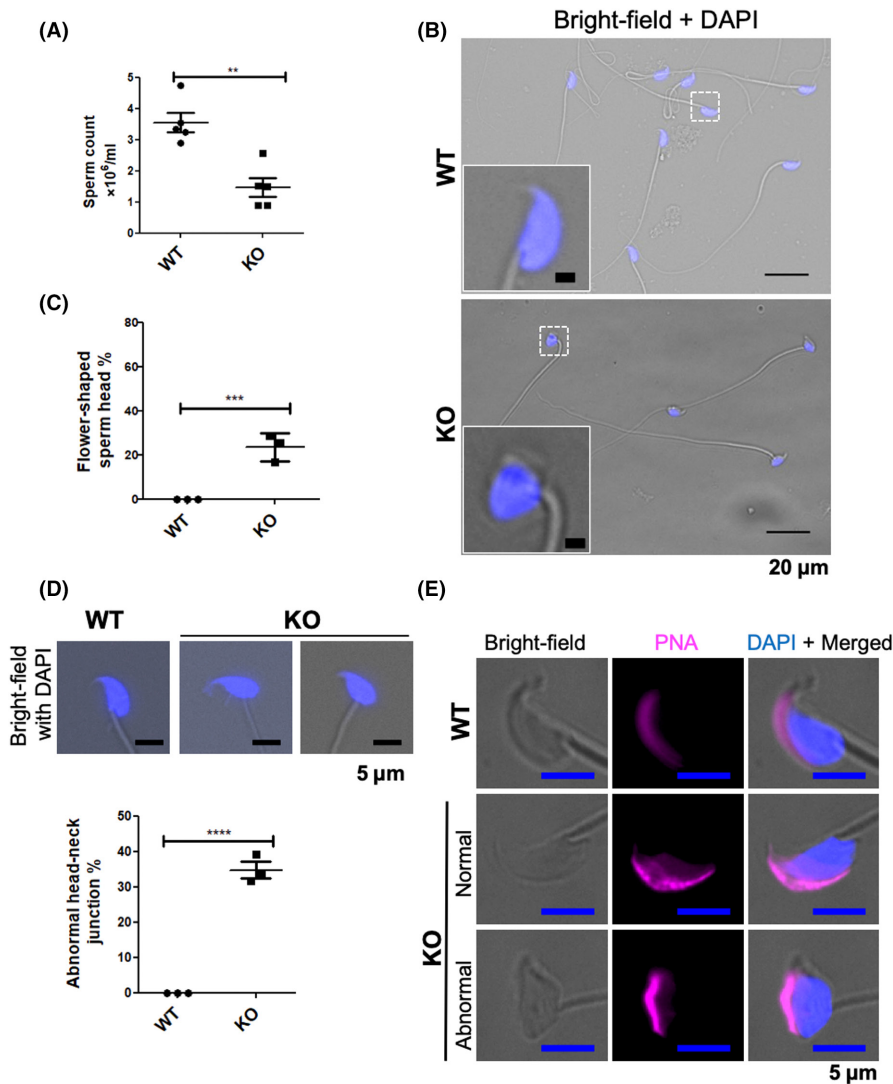
FIGURE 4 TSNAXIP1 deficiency induces oligospermia and sperm head deformity. (A). Number of cauda epididymal sperm in WT and KO mice at 10 weeks of age ($n = 5$). (B). Morphology of WT and KO cauda epididymal sperm. Scale bar 20 μm. Insets show high magnification. Scale bar 2 μm. (C). Percentage of flower-shaped sperm heads in WT and KO ($n = 3$). (D). Percentage of abnormal head–neck junction in WT and KO sperms ($n = 3$) and representative images. Scale bar 5 μm. Data are presented as mean ± SEM. **$p < 0.01$, ***$p < 0.001$, ****$p < 0.0001$. (E). Acrosome formation was visualized in WT and KO sperm by PNA staining (magenta). Scale bar 5 μm.

differences in phenotypes between their study and this study. The size of testes, sperm count, and sperm morphology were affected by the lack of TSNAXIP1 in this study, whereas those were not affected in the previous study. On the other hand, both TSNAXIP1 deleted mice in the previous study and this study were subfertile despite spermatogenesis in both was normal. In the previous study, the ratio of motile sperm in TSNAXIP1 null male was reduced. Moreover, an asymmetric waveform of flagellar beating of TSNAXIP1 null spermatozoa was observed, which might be the reason of circular motion and ultimately reducing the progressive motility of TSNAXIP1 null spermatozoa. The difference between the previous study and this study is deleted region in the TSNAXIP1 genome. The genome including exon 4 and most of exon 5 in TSNAXIP1 was removed in this study, whereas the genome from exon 3 to exon 13 was removed in the previous study. A sequencing of *Tsnaxip1* transcript expressed in the TSNAXIP1 deleted testis generated in this study revealed that a truncated form of TSNAXIP1 consisting of 83aa without SMC and TSNAXIP_N domains could be expressed (Figure S4C), while the SMC domain of TSNAXIP1 was completely disappeared (Figure 2E). Although the antibody used in this study could not recognize the

truncated form of TSNAXIP1, an expression of the short form of TSNAXIP1 could not be confirmed. The short TSNAXIP1 could have a dominant negative effect against wildtype TSNAXIP1 and could induce abnormal morphology of sperm heads. However, an immuno-blotting experiment showed that TSNAXIP1 was present in sperm tails but not in sperm heads in the previous study.[16] The short form of TSNAXIP1 could alter its localization from tails to heads and could induce abnormal head morphology. A newly developed antibody which can recognize the short form of TSNAXIP1 could be required to reveal a possibility of the alternative localization of the short form of TSNAXIP1.

Otherwise, dominant negative effect of the short TSNAXIP1 might be exhibited during spermatogenesis, since TSNAXIP1 null testes and seminiferous tubules were smaller and TSNAXIP1 could be involved in functions of intercellular bridge. TSNAXIP1 has been reported to interact with TSNAX, which associates with TSN. TSN is a DNA-binding protein and, together with TSNAX, plays roles in a variety of cellular activities including cell division, DNA damage response and microRNA (miRNA) degradation during dicer deficiency.[9,17–19] Although expression of TSNAX protein disappeared

in TSN-null mice,[11] the expression levels of *Tsn* and *Tsnax* transcripts in testes were not changed by the lack of TSNAXIP1 in this study (Figure 2E), suggesting that both TSN and TSNAX could be still active in TSNAXIP1 KO spermatogenesis. Since TSN-TSNAX complex cannot inhibit the formation of flower-like head shape of TSNAXIP1 null sperm, TSNAXIP1 could have an independent function from TSN-TSNAX complex during spermatogenesis. A functional involvement of TSNAXIP1 in intercellular bridge could be required to reveal if a dominant negative effect of the short form of TSNAXIP1 induces flower-like head shape of sperm and a reduced area of seminiferous tubules through an altered function of intercellular bridges.

Taken all together, we found TSNAXIP1 as a testis-expressed gene and disruption of TSNAXIP1 causes severe oligospermia, which leads to sub-fertility in male mice. TSNAXIP1 could have specific roles in spermiogenesis, particularly in the formation of sperm head. Since TSNAXIP1 is highly conserved between mouse and human, further analyses of TSNAXIP1 function and genetic analyses of human infertile patients might be useful to understand the pathogenesis of human infertility.

CONFLICT OF INTEREST STATEMENT
The authors declare no conflict of interest.

ETHICAL APPROVAL
All mouse experiments were performed in accordance with the protocol approved by the Institutional Animal Care and the Ethics Committee on Animal Experiments at Kyushu University (#A22-288-1).

ORCID
Naoki Iwamori https://orcid.org/0000-0001-5903-8386

REFERENCES
1. Kuchakulla M, Narasimman M, Khodamoradi K, Khosravizadeh Z, Ramasamy R. How defective spermatogenesis affects sperm DNA integrity. Andrologia. 2021;53(1):e13615.
2. Shima JE, McLean DJ, McCarrey JR, Griswold MD. The murine testicular transcriptome: characterizing gene expression in the testis during the progression of spermatogenesis. Biol Reprod. 2004;71(1):319–30.
3. O'Donnell L. Mechanisms of spermiogenesis and spermiation and how they are disturbed. Spermatogenesis. 2014;4(2):e979623.
4. Pineau C, Hikmet F, Zhang C, Oksvold P, Chen S, Fagerberg L, et al. Cell type-specific expression of testis elevated genes based on transcriptomics and antibody-based proteomics. J Proteome Res. 2019;18(12):4215–30.
5. Bray JD, Chennathukuzhi VM, Hecht NB. Identification and characterization of cDNAs encoding four novel proteins that interact with translin associated factor-X. Genomics. 2002;79(6):799–808.
6. Banu Y, Matsuda M, Yoshihara M, Kondo M, Sutou S, Matsukuma S. Golgi matrix protein gene, Golga3/Mea2, rearranged and re-expressed in pachytene spermatocytes restores spermatogenesis in the mouse. Mol Reprod Dev. 2002;61(3):288–301.
7. Ding X, Xu R, Yu J, Xu T, Zhuang Y, Han M. SUN1 is required for telomere attachment to nuclear envelope and gametogenesis in mice. Dev Cell. 2007;12(6):863–72.
8. Wu S, Li L, Wu X, Wong CKC, Sun F, Cheng CY. AKAP9 Supports spermatogenesis through its effects on microtubule and Actin cytoskeletons in the rat testis. FASEB J. 2021;35(10):1–24.
9. Ishida R, Okado H, Sato H, Shionoiri C, Aoki K, Kasai M. A role for the octameric ring protein, Translin, in mitotic cell division. FEBS Lett. 2002;525(1–3):105–10.
10. Morales CR, Lefrancois S, Chennathukuzhi V, El-Alfy M, Wu XQ, Yang J, et al. A TB-RBP and Ter ATPase complex accompanies specific mRNAS from nuclei through the nuclear pores and into intercellular bridges in mouse male germ cells. Dev Biol. 2002;246(2):480–94.
11. Chennathukuzhi V, Stein JM, Abel T, Donlon S, Yang S, Miller JP, et al. Mice deficient for testis-brain RNA-binding protein exhibit a coordinate loss of TRAX, reduced fertility, altered gene expression in the brain, and behavioral changes. Mol Cell Biol. 2003;23(18):6419–34.
12. Lybaert P, Danguy A, Leleux F, Meuris S, Lebrun P. Improved methodology for the detection and quantification of the acrosome reaction in mouse spermatozoa. Histol Histopathol. 2009;24(8):999–1007.
13. Wei YL, Yang WX. The acroframosome-acroplaxome-manchette axis may function in sperm head shaping and male fertility. Gene. 2018;660:28–40.
14. Nasmyth K, Haering CH. The structure and function of SMC and kleisin complexes. Annu Rev Biochem. 2005;74:595–648.
15. Lindemann CB, Lesich KA. Functional anatomy of the mammalian sperm flagellum. Cytoskeleton. 2016;73(11):652–69.
16. Kaneda Y, Miyata H, Shimada K, Oura S, Ikawa M. Testis-specific proteins, TSNAXIP1 and 1700010I14RIK, are important for sperm motility and male fertility in mice. Andrology. 2023; in press.
17. Kasai M, Ishida R, Nakahara K, Okumura K, Aoki K. Mesenchymal cell differentiation and diseases: involvement of translin/TRAX complexes and associated proteins. Ann N Y Acad Sci. 2018;1421(1):37–45.
18. Erdemir T, Bilican B, Oncel D, Goding CR, Yavuzer U. DNA damage-dependent interaction of the nuclear matrix protein C1D with translin-associated factor X (TRAX). J Cell Sci. 2002;115(1):207–16.

19. Asada K, Canestrari E, Fu X, Li Z, Makowski E, Wu YC, et al. Rescuing dicer defects via inhibition of an anti-dicing nuclease. Cell Rep. 2014;9(4):1471–81.

SUPPORTING INFORMATION

Additional supporting information can be found online in the Supporting Information section at the end of this article.